ISSN 0967-0912, Steel in Translation, 2018, Vol. 48, No. 10, pp. 631–636. © Allerton Press, Inc., 2018.
Original Russian Text © K.V. Aksenova, E.N. Nikitina, Yu.F. Ivanov, D.A. Kosinov, 2018, published in Izvestiya Vysshikh Uchebnykh Zavedenii, Chernaya Metallurgiya, 2018, No. 10, pp. 787–793.

Strain Hardening of Bainitic and Martensitic Steel in Compression

K. V. Aksenova[a], *, E. N. Nikitina[a], **, Yu. F. Ivanov[b, c], *, and D. A. Kosinov[a], ******

[a] *Siberian State Industrial University, Novokuznetsk, Russia*
[b] *Tomsk Polytechnic University, Tomsk, Russia*
[c] *Institute of High-Current Electronics, Siberian Branch, Russian Academy of Sciences, Tomsk, Russia*
**e-mail: 19krestik91@mail.ru*
***e-mail: nikitina_en@mail.ru*
****e-mail: yufi55@mail.ru*
*****e-mail: kosinov.dima@rambler.ru*

Received December 12, 2017

Abstract—Martensite and bainite formed in steel on heat treatment are very complex structures, resisting quantitative analysis. Often such steels are used at high static and dynamic compressive stress. Thorough analysis of their structure after various types of treatment permits their effective use in manufacturing so as to ensure the required physicomechanical properties of the product. The properties of such materials are determined by the solid-solution structure; the presence of secondary-phase nanoparticles; dislocational substructure; the type and position of different types of boundaries; and internal stress fields. Successful control of structure and phase formation and hence of the mechanical properties of the material depends on a quantitative grasp of strain hardening of steels of different structural classes on active plastic deformation. In the present work, transmission diffractional electron microscopy is used to analyze the strain hardening of 38KhN13MFA steel with martensitic structure and 30Kh2N2MFA steel with bainitic structure in active plastic deformation (compression) by up to 26 and 36%, respectively. The contributions of strain hardening associated with intraphase boundaries, dislocational substructure, carbide phases, atoms of alloying elements, and long-range stress fields are considered. The main contributors to the strain hardening of quenched 38KhN13MFA steel are substructural hardening associated with internal long-range stress fields; and solid-solution strengthening associated with carbon atoms. For normalized 30Kh2N2MFA steel, the strain hardening may again be attributed to internal stress fields, the introduction of carbon atoms in the ferrite lattice, and also structural fragmentation when the strain exceeds 26%. The dislocational substructure and carbide particles make relatively small contributions to the hardening of such steels. The loss of strength of bainitic steel at deformation exceeding 15% is due to activation of deformational microtwinning.

Keywords: steel, martensite, bainite, strain hardening, microtwinning

DOI: 10.3103/S0967091218100029

INTRODUCTION

In the past decade, research interest in quantitative assessment of steels' physical properties had grown. Analysis of microstructures provides considerable information regarding the mechanical properties of steels [1–5]. Attention has focused, in particular, on steel strength, which may in many cases be predicted with sufficient reliability from the known alloy composition and microstructure [1, 5].

Strengthening is often studied on physical models. Empirical or semiempirical assumptions are used in some cases, especially when we need to describe the properties of complex microstructures formed in the steel (martensite or bainite).

Research has shown that martensitic or bainitic structure is responsible for the excellent physicomechanical properties of structural steels, which are widely used in industry [6–8].

We must understand the strengthening process if we are to make successful use of the steels' strength and to obtain an optimal set of properties. In addition, we need to know the key factors that control the strengthening process and their influence on many other properties, especially the ductility and plasticity.

In the present work, we analyze the strengthening of steels with bainitic and martensitic structures at different stages of plastic deformation.

EXPERIMENTAL MATERIALS AND METHODS

We investigate 38KhN13MFA and 30Kh2N2MFA structural steels [9]. After austenitization at 960°C for

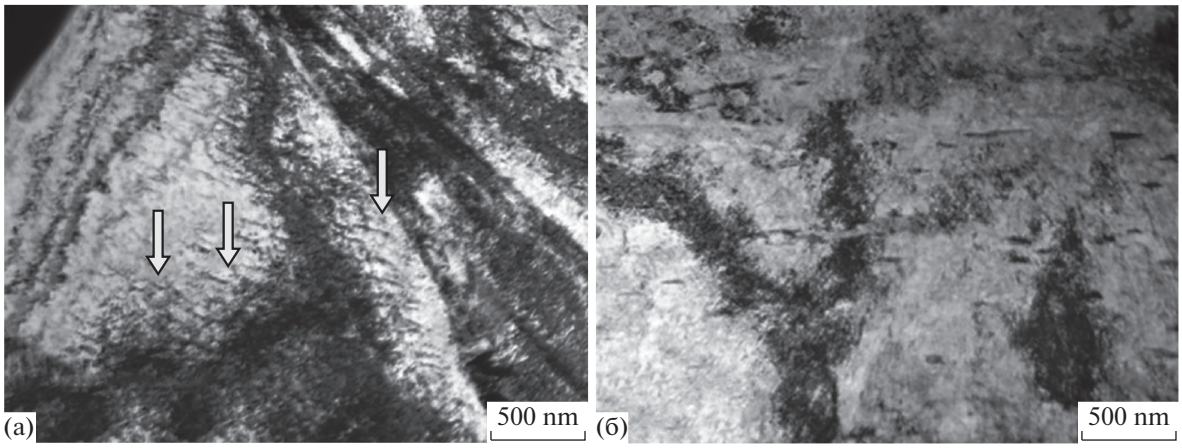

Fig. 1. Electron-microscope images of the structure in 38KhN13MFA steel (a) and 30Kh2N2MFA steel (b) prior to deformation. The arrows indicate cementite particles in packet martensite crystals.

1.5 h, 38KhN13MFA steel is cooled in water, while and 30Kh2N2MFA steel is cooled in air. Steel samples (4 × 4 × 6 mm columns) with bainitic and martensitic structures are deformed at room temperature by uniaxial compression, with different strain ε, at a rate of 7×10^{-3} s^{-1} on an Instron-1185 test machine; the load and elongation are recorded automatically. The structure and phase composition of the steel are investigated by the transmission diffractional electron microscopy of thin foil [10–12]. The determination of the structural parameters from the electron-microscope images was described in detail in [13–16].

RESULTS AND DISCUSSION

We conclude from the electron-microscope images that, after heat treatment, packet (rack) martensite is formed by shear $\gamma \rightarrow \alpha$ transformation in 38KhN13MFA steel (Fig. 1a); analogously lower-bainitic structure is formed in 30Kh2N2MFA steel (Fig. 1b). The racks include cementite particles (larger in 30Kh2N2MFA steel with bainitic structure) and dislocational substructure of grid type. The scalar density of the dislocations is about 1×10^{11} cm^{-2} in 38KhN13MFA steel, as against ~0.7×10^{11} cm^{-2} in 30Kh2N2MFA steel. The structure and phase composition of the steel and the parameters characterizing the behavior of the structure on deformation were described in more detail in [17–20].

The contributions of slowing of the dislocations on cementite particles, scaffold dislocations, and intraphase boundaries and also by interaction with internal stress fields may be estimated on the basis of the structural data in [17–20]. The contributions of different processes to the strengthening and total strength of the steels are estimated at different stages of strain hardening. That permits analysis of the evolution of the strengthening processes and the steel strength as a function of the strain. In the initial state, the crystals of martensite and lower bainite are fragmented. In other words, they are divided into regions with small-angle disorientation. Research shows that the longitudinal dimensions of the fragments in the martensite crystals are considerably greater than in crystals of lower bainite. Deformation of the steel is associated with decrease in longitudinal dimensions of the fragments as a result of the appearance of subboundaries. This process is more intense in martensite crystals. In 30Kh2N2MFA steel with $\varepsilon > 26\%$, the decrease in mean fragment size practically stops. We may assume that the fragment size reaches some critical value (about 200 nm).

The strengthening of steel by small-angle boundaries (substructural strengthening, strengthening by plate and fragment boundaries) may be estimated on the basis of Hall–Petch equation [21]

$$\sigma(L) = \sigma_0 + kL^{-m}, \quad (1)$$

where $m = 1$ or $1/2$; L is the effective size of the ferrite plates and fragments and is determined by the effective slip-plane length in the bainite or martensite plate.

When $m = 1$, we find that k varies from 0.015 to 0.010 kgf/mm; when $m = 1/2$, k varies from 0.20 to 0.98 $kgf/mm^{3/2}$ [22, 23].

In the calculations, we use the following parameter values: $k = 0.015$; $m = 1$. We assume that L is the mean longitudinal dimension of the fragments. The first term γ_0 in Eq. (1) is the frictional stress of the lattice—that is, the stress required for motion of the dislocations in pure single crystals (for example, the Peierls force for pure metals). For steels, we usually assume that $\sigma_0 = 30$–40 MPa [13].

Table 1 presents the contribution of internal boundaries (boundaries of grains, packets, martensite crystals, and fragments) to the strain hardening of steels with martensitic and bainitic structure, as a function of the strain. It is evident that, with increase

Table 1. Contributions to the yield point for martensitic and bainitic steel with different strain

Factor	Contribution to stress, MPa, for different ε (%)						
	martensitic steel			bainitic steel			
	0	10	26	0	10	26	36
$\Delta\sigma(L)$: contribution of interphase boundaries	440	450	480	300	320	600	800
$\Delta\sigma(\rho)$: contribution of dislocational substructure	290	340	360	275	320	350	360
$\Delta\sigma(h)$: contribution of long-range stress fields	280	700	900	425	554	660	733
$\Delta\sigma$(cp): contribution of carbide particles	200	300	280	260	220	250	210
$\Delta\sigma(C)$: contribution of atoms of alloying elements	660	790	800	490	570	630	740

in strain, the strengthening by fragment boundaries increases. That increase is more intense for bainitic structure, as a result of decrease in mean size of the fragments.

Plastic deformation of the steels increases the scalar dislocation density to 1.3×10^{11} cm^{-2}. The type of dislocational substructure is unchanged.

The stress required to maintain the plastic deformation—that is, the yield point σ—is related to the dislocation density as follows [1, 2, 23]

$$\sigma = \sigma_0 + k\sqrt{\rho},$$

Here σ_0 is the yield point due to nondislocational factors (other strengthening mechanisms); ρ is the mean (scalar) dislocation density; $k = m\alpha Gb$; m is the Schmid orientational factor; α characterizes the interaction between dislocations (α = 0.1–0.51 [24]); G is the shear modulus ($G \approx 80$ GPa); and b is the Burgers vector of the dislocation ($b = 0.25$ nm).

For steels, taking account of the orientational factor m, we usually assume that $m\alpha \approx 0.5$.

With increase in ε, the contribution of the scalar dislocation density to the strain hardening increases in proportion to the increase in scalar dislocation density; specifically, it increases from 275–290 MPa to 360 MPa (Table 1).

Long-range stress fields due to the defects in the steel make an important contribution to the attainment of the yield point, the strain hardening, and the failure of crystalline materials [2, 25–27].

The magnitude of the long-range stress fields is estimated on the basis of the formula [22]

$$\sigma(h) = \alpha_c Gb\sqrt{\rho_\pm} = \alpha_c Gb \sqrt{\frac{1}{b}\frac{\partial\varphi}{\partial\ell}} = \alpha_c G\sqrt{\frac{0.017b}{h}}, \quad (2)$$

where $\alpha_c = 1$ is the Strunin coefficient [28]; and h is the mean transverse dimension of the flexural extinction contour.

The mean transverse dimensions of the contours decrease with increase in the strain of the steel, according to the research in [17–20]. According to Eq. (2), the long-range internal stress fields will increase. This may be attributed to the increase in curvature and torsion of the steels' crystal lattice on account of the incompatible deformation of the martensite and bainite crystals and the carbide grains and particles. This contribution increases considerably in the range 280–900 MPa for martensitic steel and 425–733 MPa for bainitic steel.

As already noted, the steel before deformation includes iron-carbide (cementite) plates (needles). The evolution of the carbide phase on plastic deformation was considered in detail in [18, 19]. The particles obstruct the motion of dislocations, with consequent increase in strength of the steel. The strengthening depends significantly on whether the particles in the material are coherent or incoherent. The dimension D_{cr} is critical for particle intersection [29]

$$D_{cr} = \frac{4G_m b^2}{0.33\pi b_p G_p}.$$

Here G_p is the shear modulus of the particle; b_p is the Burgers vector of the dislocations moving in the particle.

For most particles present in steel, $D_{cr} \le 5$ nm. Large particles are not intersected by moving dislocations.

In the initial steels, the dimensions of the cementite particles before deformation exceed D_{cr}, according to the research in [17–20]. Hence, if we take account of the presence of cementite particles, the strengthening of the steels on deformation may be estimated from the relation derived for incoherent deposits in [30]

$$\sigma_{in} = M\frac{mG_m b}{2\pi(|\lambda - D|)}\Phi\ln\left(\left|\frac{\lambda - D}{4b}\right|\right).$$

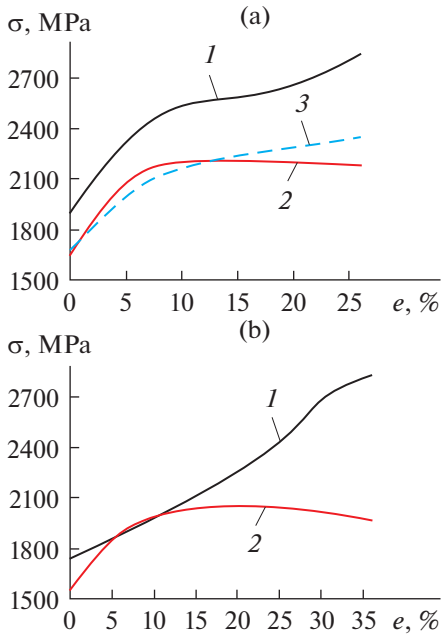

Fig. 2. Theoretical (*1*, *3*) and experimental (*2*) strain-hardening curves of 38KhN13MFA steel (a) and 30Kh2N2MFA steel (b): (—) linear summation of contributions to the strain hardening; (---) quadratic summation of two comparable contributions (long-range stress fields and solid-solution strengthening).

Here λ is the mean distance between the particles; D is the mean particle size; m is an orientational factor ($m = 2.75$ for bcc materials [31]); $\Phi = 1$ for helical dislocations and $\Phi = (1 - \nu)^{-1}$ for edge dislocations; the parameter M takes account of the nonuniform distribution of particles in the matrix ($M = 0.81$–0.85) [30].

On the basis of Table 1, we may conclude that this contribution increases from 200 to 300 MPa with increase in the strain of 38KhN13MFA steel to 10%. With further increase in ε, the contribution of cementite particles to the strengthening declines, since they dissolve. For 30Kh2N2MFA steel, this contribution varies in a complex manner between 260 and 210 MPa. That may be due to solution and repeated deposition of the cementite particles on deformation.

As a result of the presence of carbon atoms in the steels and their introduction in the crystal lattice, it is asymmetrically distorted. That facilitates significant strengthening of the material. On the assumption that the contributions of individual alloying elements to the strengthening may be added, approximate empirical formulas of the following type are usually employed in calculating the solid-solution strengthening of complex alloy steels [1, 13]

$$\sigma_r = \sum_{i=1}^{m} (k_i c_i). \qquad (3)$$

Here k_i is the strengthening coefficient of ferrite, expressed as the increment in the yield point when 1 wt % of alloying element i is dissolved; and c_i is the concentration of element i dissolved in the ferrite, wt %. The value of k_i for different elements is determined experimentally [1, 13].

For quenched 38KhN13MFA steel, the contribution to the yield point associated with the presence of interstitial atoms (carbon) and substitutional atoms (nickel, chromium, molybdenum, and vanadium) according to Eq. (3) increases within the range 660–800 MPa with increase in ε; for 30Kh2N2MFA steel, this contribution increases from 490 to 740 MPa (Table 1). That may be attributed to the solution of cementite particles, the introduction of some of carbon atoms in the iron lattice, and deposition on dislocations.

If we compare the contributions to the strain hardening of the steels (Table 1), we find that the long-range stress fields and solid-solution strengthening make the greatest contribution to the strengthening for the martensitic steel. The contribution of the long-range stress fields increases with increase in ε, while the contribution of long-range stress fields increases sharply in the initial stages of deformation and then saturates at ε = 10%. The other contributions hardly change with increase in ε and are much smaller than the other two. For the bainitic steel, long-range stress fields and solid-solution strengthening make about the same contribution to the strengthening; in the final stage (when ε > 26%), substructural hardening (strengthening of the intraphase boundaries) plays an equal role.

The overall yield point of the steel may be expressed as the linear sum of the contributions of the individual strengthening mechanisms [1, 13, 32, 33]

$$\sigma = \Delta\sigma_0 + \Delta\sigma(L) + \Delta\sigma(\rho) + \Delta\sigma(h) + \Delta\sigma(\mathrm{cp}) + \Delta\sigma(C),$$

where $\Delta\sigma_0$ is the contribution associated with friction of the matrix lattice; $\Delta\sigma(L)$ is the contribution of interphase boundaries; $\Delta\sigma(\rho)$ is the contribution of dislocational substructure; $\Delta\sigma(h)$ is the contribution of long-range stress fields; $\Delta\sigma(\mathrm{cp})$ is the contribution of carbide particles; and $\Delta\sigma(C)$ is the contribution of atoms of the alloying elements.

Addition of the contributions assumes that each process acts independently on the yield point of the material.

In Fig. 2, we show calculated (*1*, *3*) and experimental *2*) strain-hardening curves for martensitic and bainitic steels. We see that the σ– ε curves *1* calculated additively are significantly higher than the experimental curves *2* when ε > 15%. With increase in ε, the discrepancy increases.

We may assume that this discrepancy for bainitic steel, which is most significant at large ε, is due to the

role of microtwinning in the deformation of steel, as established in [34]. When $\varepsilon = 5$ and 10%, there is little deformational twinning of the steel, according to [19, 20]. With increase in ε, deformational twinning extends over a significantly greater volume of material. Therefore, we may conclude that muicrotwinning is responsible for orientational weakening of the steel and facilitates slip of the dislocations.

For steel with martensitic structure, the strain-hardening curve is also calculated by quadratic summation of two comparable contributions ($\Delta\sigma_1 \approx \Delta\sigma_2$), as proposed in [1, 3, 35]

$$\sigma = \sqrt{\Delta\sigma_1^2 + \Delta\sigma_2^2}.$$

We see that, with linear summation of the contributions (Fig. 2a, curve *1*), the discrepancy between the calculated and experimental curves is as much as 700 MPa. With quadratic summation of the contributions of long-range stress fields and solid-solution strengthening (Fig. 2a, curve *3*), the calculated and experimental curves are in qualitative agreement; the discrepancy is no greater than 150 MPa.

CONCLUSIONS

Quantitative analysis of the structure of steel with martensitic and bainitic structure subjected to uniaxial compressive deformation permits assessment of the various contributions to strain hardening. Analysis of the strain hardening of steels shows that many factors are responsible.

The greatest contributors to strain hardening are long-range internal stress fields and solid-solution strengthening due to the introduction of carbon atoms in the ferrite lattice. For bainitic steel, at large strain, the contribution of intraphase boundaries increases.

ACKNOWLEDGMENTS

Financial support was provided by the Russian Foundation for Basic Research (grant 16-08-00385-a) and by a stipend from the Russian President for young scientists involved in research that contributes to economic modernization (project SP 1335.2016.1).

REFERENCES

1. Pickering, F.B., *Physical Metallurgy and the Design of Steels*, London: Applied Science, 1978.
2. Shtremel', M.A., *Prochnost' splavov. Chast' II. Deformatsiya. Uchebnik dlya vuzov* (Strength of Alloys, Part 2: Deformation. Manual for Higher Education Institutions), Moscow: Mosk. Inst. Stali Splavov, 1997.
3. Gromov, V.E., Kozlov, E.V., Bazaikin, V.I., Tsellermaer, V.Ya., Ivanov, Yu.F., et al., *Fizika i mekhanika volocheniya i ob"emnoi shtampovki* (Physics and Mechanics of Drawing and Large Forging), Moscow: Nedra, 1997.
4. Kelly, A. and Nicholson, R.B., *Strengthening Methods in Crystals*, Amsterdam: Elsevier, 1971.
5. Fleischer, R.L. and Hibberd, W.R., *The Relation Between the Structure and Mechanical Properties of Metals*, London: Her Majesty's Stationary Off., 1963.
6. Kurdyumov, V.G., Utevskii, L.M., and Entin, R.I., *Prevrashcheniya v zheleze i stali* (Transformations in Iron and Steel), Moscow: Nauka, 1977.
7. Sourmail T. and Smanio V., Low temperature kinetics of bainite formation in high carbon steels, *Acta Mater.*, 2013, vol. 61, no. 7, pp. 2639–2648.
8. Borgenstam, A., Hillert, M., and Agren, J., Metallographic evidence of carbon diffusion in the growth of bainite, *Acta Mater.*, 2009, vol. 57, no. 11, pp. 3242–3252.
9. Pridantsev, M.V., Davydova, L.N., and Tamarina, A.M., *Konstruktsionnye stali: Spravochnik* (Structural Steels: Handbook), Moscow: Metallurgiya, 1980.
10. Egerton, R.F., *Physical Principles of Electron Microscopy: An Introduction to TEM, SEM, and AEM*, Berlin: Springer-Verlag, 2005.
11. Kumar, C.S.S.R., *Transmission Electron Microscopy: Characterization of Nanomaterials*, New York: Springer-Verlag, 2014.
12. *Transmission Electron Microscopy: Diffraction, Imaging, and Spectrometry*, Carter, C.B. and Williams, D.B., Eds., Berlin: Springer-Verlag, 2016.
13. Gol'dshtein, M.I. and Farber, B.M. *Dispersionnoe uprochnenie stali* (Disperse Hardening of Steel), Moscow: Metallurgiya, 1979.
14. Hirsch, P.B., Howie, A., Nicholson, R.B., Pashley, D.W., and Whelan, M.J., *Electron Microscopy of Thin Crystals*, Washington: Butterworth, 1965.
15. Chernyavskii, K.S., *Stereologiya v metallovedenii* (Stereology in Metal Science), Moscow: Metallurgiya, 1977.
16. Utevskii, L.M., *Difraktsionnaya elektronnaya mikroskopiya v metallovedenii* (Diffraction Electron Microscopy in Metal Science), Moscow: Metallurgiya, 1973.
17. Ivanov, Yu.F., Kolubaeva, Yu.A., Kornet, E.V., and Gromov, V.E., Formation of the fine structure and phase composition of structural steel on quenching, *Steel Transl.*, 2009, vol. 39, no. 4, pp. 302–306.
18. Ivanov, Yu.F., Kornet, E.V., Gromov, V.E., and Konovalov, S.V., Structural-phase transformations in hardened structural steel under deformation, *Usp. Fiz. Met.*, 2009, vol. 10, no. 4, pp. 391–416.
19. Gromov, V.E., Nikitina, E.N., and Ivanov, Yu.F., Evolution of carbide and defective subsystems of steel with bainitic structure under deformation, *Probl. Chern. Met. Materialoved.*, 2015, no. 3, pp. 74–80.
20. Gromov, V.E., Nikitina, E.N., Ivanov, Yu.F., and Aksenova, K.V., Regularities of bainitic steel deformation transition, *IOP Conf. Ser.: Mater. Sci. Eng.*, 2016, vol. 150, art. ID 012025.
21. Naylor, I.R., The influence of the lath morphology on the yield stress and transition temperature of martensitic-bainitic steels, *Metall. Trans. A*, 1979, vol. 10, no. 7, pp. 861–873.
22. Belen'kii, B.Z., Farber, B.M., and Gol'dshtein, M.I., Estimates of the strength of low-carbon low-alloy steels

according to their structural data, *Fiz. Met. Metalloved.*, 1975, vol. 39, no. 3, pp. 403–409.

23. Trefilov, V.I., Moiseev, V.I., Pechkovskii, E.P., et al., *Deformatsionnoe uprochenie i razrushenie polikristallicheskikh metallov* (Deformation Hardening and Destruction of Polycrystalline Metals), Kiev: Naukova Dumka, 1987.
24. McLean, D., *Mechanical Properties of Metals*, London: Wiley, 1962.
25. Koneva, N.A. and Kozlov, E.V., Nature of substructural hardening, *Sov. Phys. J.*, 1982, vol. 25, no. 8, pp. 681–691.
26. Koneva, N.A. and Kozlov, E.V., Physics of sub-structural hardening, *Vestn. Tomsk. Gos. Arkh.-Stroit. Univ.*, 1999, no. 1, pp. 21–35.
27. Kocks, U.F., Statistical treatment of penetrable obstacles, *Can. J. Phys.*, 1967, vol. 45, no. 2, pp. 737–755.
28. Strunin, B.M., Probabilistic description of the field of internal stresses with random arrangement of dislocations, *Fiz. Tverd. Tela*, 1971, vol. 13, no. 3, pp. 923–926.
29. Mott, N.F. and Nabarro, F.R.N., The distribution of dislocations in slip band, *Proc. Phys. Soc.*, 1940, vol. 52, no. 1, pp. 86–93.
30. Ashby, M.F., *Physics of Strength and Plasticity*, Cambridge, Ma: MIT Press, 1969.
31. Tekin, E. and Kelly, P.M., *Precipitation from Iron-Base. Alloys*, London: Gordon and Breach, 1965.
32. Norstrom, L.A., On the yield strength of quenched low-alloy lath martensite, *Scand. J. Metall.*, 1976, vol. 5, no. 4, pp. 159–165.
33. Prnka, T., Quantitative relationships between the parameters of dispersed precipitates and the mechanical properties of steels, *Met. Sci. Heat Treat.*, 1975, vol. 17, no. 7, pp. 548–552.
34. Kiseleva, S.F., Popova, N.A., Koneva, N.A., and Kozlov, E.V., Influence of transformation microtwines on excessive density of dislocations and internal stresses of deformed FCC material, *Izv. Ross. Akad. Nauk, Ser. Fiz.*, 2012, vol. 76, no. 13, pp. 70–74.
35. Orowan, E., Conditions for dislocation passage of precipitates, *Proc. Symp. Int. "Stress in Metals and Alloys,"* London: Inst. Met., 1948, pp. 451–454.

Translated by Bernard Gilbert

SPELL: 1. ok